Optimization of mid-frequency vibration for complex built-up systems using hybrid FE-SEA method

Ruxin Gao[a], Yahui Zhang[a*], David Kennedy[b]

[a] *State Key Laboratory of Structural Analysis for Industrial Equipment, Department of Engineering Mechanics, International Center for Computational Mechanics, Dalian University of Technology, Dalian 116023, PR China*

[b] *School of Engineering, Cardiff University, Cardiff CF24 3AA, Wales, UK*

Corresponding author:

Dr. Y. H. Zhang

State Key Laboratory of Structural Analysis for Industrial Equipment, Department of Engineering Mechanics, Dalian University of Technology, Dalian 116023, PR China

Email: zhangyh@dlut.edu.cn

Tel: +86 411 84706337

Fax: +86 411 84708393

Abstract

This paper deals with the sensitivity analysis of dynamic response and optimal size design of complex built-up systems in the mid-frequency range. A complex built-up system may be fabricated from many components which often differ greatly in materials and sizes. It may be subjected to many different wavelength structural deformations and may typically exhibit mixed mid-frequency behavior which is very sensitive to uncertainties at higher frequencies. In order to perform optimization on the mid-frequency vibration of the complex built-up systems, the hybrid Finite Element (FE) - Statistical Energy Analysis (SEA) method, in which the deterministic and statistical subsystem are respectively modeled by using FE and SEA, is implemented in the present work. In the optimization model, the size parameters of the deterministic and statistical subsystems are taken as design variables. The energy of the system under a specific frequency, or the frequency-aggregated energy of the system in a given frequency band, is taken as the objective function to be minimized. In this context, an efficient direct differentiation method for sensitivity analysis is derived. Then the optimization problem is solved by using a gradient-based mathematical programming algorithm. Two numerical examples illustrate the efficiency and effectiveness of the proposed method. The energy level of the complex built-up system, whether at a single frequency or in a given frequency band, can be significantly improved through optimization.

Keywords: Mid-frequency; Dynamic optimization; Hybrid FE-SEA method; Complex

built-up system; Sensitivity analysis

1 Introduction

Complex built-up systems such as stiffened panels are widely used in aircraft, automobiles and ships, and their layout, shape and size directly affect the dynamic performance of the engineering structures. Therefore, the dynamic optimum design of complex built-up systems has long been a challenging subject in structural design, and has been widely addressed by academia and industry. Initially, researchers focused their attention on static optimization of structures because of the difficulty of performing dynamic optimization. Zarghmee (1968) and Taylor (1968) proposed the concept of the optimum frequency of structures, and many researchers studied the optimization of natural frequencies. Comparatively, there were fewer studies on dynamic response optimization for structures at that time. Karnopp and Trikka (1969), Sevin and Walter (1971) and Afiminiwala and Mayne (1974) proposed the optimization of transient response for engineering structures. Since then, the study of dynamic response optimization design has gradually increased (Hsieh and Arora 1984; Kang, Park, and Arora 2006). In recent years, topology optimization has attracted more attention than sizing and shape optimization and has been widely applied in many fields (Bendsøe and Sigmund 2003; Du and Olhoff 2007; Dühring and Jensen 2008; Zhang and Kang 2014).

It is very important to correctly obtain the dynamic response of structures, since the

structural analysis is essential for structural optimization. The studies mentioned above used deterministic methods, such as the Finite Element (FE) method (Bathe 1996; Zienkiewicz and Taylor 2000) to study the deterministic optimization of structures in the low-frequency domain. Complex built-up engineering systems such as automobiles and aircraft may be subjected to a wide range of excitation frequencies during their operation. The deformation wavelength of components of a system will decrease remarkably as the frequency increases. In the context of the FE method, there are two problems that cannot be ignored (Mace and Shorter 2000; Desmet 2002; Cotoni, Shorter, and Langley 2007): 1) A very fine finite element mesh is required to capture the short wavelength deformations of a system, which leads to a high number of degrees of freedom, so that the FE model is often computationally expensive. 2) The response of a system becomes sensitive to uncertainties which inevitably arise during the manufacture and assembly of the system.

Systems with the same nominal parameters may have different responses. Hence, the optimum design of a system in the mid-frequency range may not be achieved by deterministic methods. As a popular statistical method, Statistical Energy Analysis (SEA) (Lyon and DeJong 1995), which considers the uncertainties of the system, can give a good prediction for the statistical behavior of the system at higher frequencies with little time cost. However, the assumptions (Langley 1989; Lyon and DeJong 1995) introduced in SEA were numerous: 1) The coupling between the subsystems is weak. 2) The power

transmitted is proportional to the difference of the modal energies between the coupled subsystems. 3) The subsystem has enough modes in the frequency band of interest. 4) The modal overlap of the subsystem is high enough. 5) Every resonant mode in a subsystem is equally energetic. The above assumptions may not be satisfied when the system is subjected to long-wavelength deformation at lower frequencies (Langley 1989).

A complex built-up system fabricated from many components which differ greatly in materials and sizes may be subjected to many different wavelength deformations and may typically exhibit mixed mid-frequency behavior which is very sensitive to uncertainties at higher frequencies. In the context of mid-frequency vibration, the vibration behavior of the system may not be properly described by simply using FE or SEA. To address this situation, many improved methods have been proposed. These methods may be simply divided into three types. The first type aims to improve the deterministic method, e.g. using FE reduction techniques (Soize 1998; Hinke, Dohnal, and Mace 2009; Kassem, Soize, and Gagliardini 2011), high-order FE methods (Harari and Avraham 1997; Wilcox et al. 2010), stochastic FE analysis (Vanmarcke and Grigoriu 1983; Yamazaki, Shinozuka, and Dasgupta 1988; Van Vinckenroy and De Wilde 1995) and analytical or semi-analytical analysis based on wave methods (Langley 1989; Ladevèze and Arnaud 2000; Duhamel, Mace, and Brennan 2006; Pluymers et al. 2007; Ma, Zhang, and Kennedy 2015). The second type (Keane and Price 1987; Langley 1992; Le Bot 1998; Mace 1994, 2005; Maxit and Guyader 2003; Tanner 2009) addresses the

applicability of the assumptions in SEA. These two types of improved methods extend the effective frequency range for analysis using traditional methods. Considering the different vibration behaviors of the components of the system when it is excited in mid-frequency ranges, the third type (Zhao and Vlahopoulos 2000; Shorter and Langley 2005b; Ji, Mace, and Pinnington 2006; Vergote et al. 2011; Zhu et al. 2014; Ma, Zhang, and Kennedy 2015) combines the deterministic and statistical methods to establish a hybrid model for mid-frequency vibration of the system. The most popular hybrid approach for the mid-frequency vibration is the hybrid FE-SEA method proposed by Shorter and Langley (2005b). In this hybrid FE-SEA method, a complex built-up system can be divided into a series of deterministic and statistical subsystems according to the deformation wavelength. The deterministic subsystem is modeled using FE, while the statistical subsystem is modeled using SEA. The dynamic coupling between the deterministic and statistical subsystems can be described as the transmission and reflection of the vibration wave. A non-iterative relationship between the two types of subsystems is established by using the diffuse-field reciprocity (Shorter and Langley 2005a). The hybrid FE-SEA method can predict the ensemble average of the response of the system, and has been extended (Langley and Cotoni 2007) to predict the ensemble variance of the response of the system. By introducing a parametric model of uncertainty in the FE component, the assumption that the FE component is deterministic was relaxed by Cicirello and Langley (2013, 2014). Muthalif and Langley (2012) studied the active

control of high-frequency vibration, exploiting the hybrid FE-SEA method to provide efficient response predictions at mid- and high-frequency ranges. The optimum skyhook damping value and its location were obtained using the MATLAB GADS toolbox with combined genetic and pattern search algorithms. As intelligent algorithms, genetic algorithms do not require sensitivity analysis and have good global searching ability. However, genetic algorithms may take longer to calculate, especially for optimization problems with many design variables.

The present work exploits the hybrid FE-SEA method to provide efficient response predictions at mid-frequency range. Then the optimization problem is solved by using a gradient-based mathematical programming algorithm. In the proposed optimization model, the ensemble average energy under a single excitation frequency, or the frequency-aggregated ensemble average energy in a given frequency band, is taken as the objective function to be minimized, and the design variables are the size parameters of the deterministic and statistical subsystems. A direct differentiation scheme for sensitivity analysis is derived. The efficiency and effectiveness of the present method are verified by two numerical examples, in which the energy level of the complex built-up system, whether at a single frequency or in a given frequency band, can be significantly decreased through optimization. The basic principles of the hybrid FE-SEA method are outlined in section 2. The optimization problem formulation under a specific excitation frequency and in a given frequency band are respectively developed in section 3 and section 4, as

well as the sensitivity analysis. In section 5, two numerical examples are presented to illustrate the validity of the proposed method. The influence of the mass constraint factor is also discussed. Finally, conclusions are given in section 6.

2 Basic principles of hybrid FE-SEA method

In the hybrid FE-SEA method, the response of the statistical subsystem is partitioned into the direct field and the reverberant field (Shorter and Langley 2005a). First, the governing equation of the system is established by considering the existence of the direct field dynamic stiffness matrix (DSM) and the blocked reverberant force. Second, the power balance equation for the reverberant field is established by considering the energy conservation of the statistical subsystem. Finally, the above two types of equations are related by the diffuse-field reciprocity principle (Shorter and Langley 2005a) which is a non-iterative relationship between the ensemble average energy of the statistical subsystem and the cross-spectrum of the blocked reverberant force associated with the reverberant field. Hence, a non-iterative hybrid approach which combines equations of dynamic equilibrium and power balance for the mid-frequency vibration of the complex built-up system is established.

2.1 Governing equation of the system

The direct field and reverberant field of the jth statistical subsystem can be viewed as two different vectors of forces, $\mathbf{f}_{\mathrm{dir}}^{(j)}$ and $\mathbf{f}_{\mathrm{rev}}^{(j)}$, respectively, acting on the deterministic

subsystem, at the coupling region of the two types of subsystems. The governing equation of the deterministic subsystem can be written as (Muthalif and Langley 2012)

$$\mathbf{D}_{\mathrm{d}}\mathbf{q} = \mathbf{f}_{\mathrm{ext}} + \sum_{j} \mathbf{f}_{\mathrm{rev}}^{(j)} - \sum_{j} \mathbf{f}_{\mathrm{dir}}^{(j)} \tag{1}$$

where $\mathbf{q}$ represents the displacements of the deterministic subsystem, and $\mathbf{f}_{\mathrm{ext}}$ is the generalized force acting on the deterministic subsystem. $\mathbf{D}_{\mathrm{d}}$ is the DSM of the deterministic subsystem and is written as $\mathbf{D}_{\mathrm{d}} = -\omega^2\mathbf{M} + \mathrm{i}\omega\mathbf{C} + \mathbf{K}$, where $\mathbf{M}$, $\mathbf{C}$ and $\mathbf{K}$ are the mass, damping, and stiffness matrices, respectively. ω is the angular frequency, and $\mathrm{i} = \sqrt{-1}$ is the imaginary unit. $\mathbf{f}_{\mathrm{dir}}^{(j)}$ can be expressed in terms of $\mathbf{D}_{\mathrm{dir}}^{(j)}$, the direct field DSM for the jth statistical subsystem, and $\mathbf{q}$, and is written as (Muthalif and Langley 2012)

$$\mathbf{f}_{\mathrm{dir}}^{(j)} = \mathbf{D}_{\mathrm{dir}}^{(j)}\mathbf{q} \tag{2}$$

Inserting Equation (2) into Equation (1) gives the following expression for the governing equation of the system (Muthalif and Langley 2012)

$$\mathbf{D}_{\mathrm{tot}}\mathbf{q} = \mathbf{f}_{\mathrm{ext}} + \sum_{j} \mathbf{f}_{\mathrm{rev}}^{(j)} \tag{3}$$

where $\mathbf{D}_{\mathrm{tot}}$ is the total DSM, which can be written as

$$\mathbf{D}_{\text{tot}} = \mathbf{D}_{\text{d}} + \sum_j \mathbf{D}_{\text{dir}}^{(j)} \tag{4}$$

The reverberant force can be expressed in terms of its square by using the diffuse-field reciprocity relationship (Shorter and Langley 2005a), as

$$\mathbf{S}_{ff}^{\text{rev}} = \langle \mathbf{f}_{\text{rev}} \mathbf{f}_{\text{rev}}^{\text{H}} \rangle = \sum_j \alpha_j \text{Im}\left\{\mathbf{D}_{\text{dir}}^{(j)}\right\} \tag{5}$$

where $\mathbf{f}_{\text{rev}} = \sum_j \mathbf{f}_{\text{rev}}^{(j)}$, $\langle \cdot \rangle$ is the ensemble average, $\cdot^{\text{H}}$ is the Hermitian transpose of $\cdot$, and

$$\alpha_j = \frac{4E_j}{\pi \omega n_j} \tag{6}$$

where E_j and n_j respectively represent the ensemble average energy and the modal density of the jth statistical subsystem (Lyon and DeJong 1995). Writing Equation (3) in cross-spectral form, averaging over an ensemble of statistical subsystems and using Equation (5) gives (Shorter and Langley 2005b)

$$\mathbf{S}_{qq} = \mathbf{S}_{qq}^{\text{ext}} + \sum_j \alpha_j \boldsymbol{\Upsilon}_{\text{dir}}^{(j)} \tag{7}$$

with

$$\mathbf{S}_{qq}^{\text{ext}} = \mathbf{D}_{\text{tot}}^{-1} \mathbf{S}_{ff}^{\text{ext}} \mathbf{D}_{\text{tot}}^{-\text{H}} \tag{8}$$

$$\boldsymbol{\Upsilon}_{\mathrm{dir}}^{(j)} = \mathbf{D}_{\mathrm{tot}}^{-1}\mathrm{Im}\left\{\mathbf{D}_{\mathrm{dir}}^{(j)}\right\}\mathbf{D}_{\mathrm{tot}}^{-\mathrm{H}} \tag{9}$$

2.2 Power balance equation of the statistical subsystems

The statistical subsystems are modeled by using SEA, and the power balance equation of the statistical subsystems are given as (Lyon and DeJong 1995)

$$\mathbf{L}\mathbf{N}^{-1}\mathbf{E} = \mathbf{P}_{\mathrm{in}}^{\mathrm{dir}} + \mathbf{P}_{\mathrm{in}}^{\mathrm{ext}} \tag{10}$$

where $\mathbf{P}_{\mathrm{in}}^{\mathrm{dir}}$ and $\mathbf{P}_{\mathrm{in}}^{\mathrm{ext}}$ are the vectors of the time and ensemble average input power to the statistical subsystems due to the contributions from the deterministic subsystem and the external excitation, respectively. $\mathbf{E}$ is the vector of the time and ensemble average energy of the statistical subsystems. $\mathbf{N}$ is a diagonal matrix with the modal densities of the statistical subsystems on the main diagonal. $\mathbf{L}$ is the influence coefficient matrix of the modal energy. The matrix $\mathbf{L}$ has dimensions $m \times m$, where m is the number of statistical subsystems, and is given by (Shorter and Langley 2005b)

$$\mathbf{L} = \begin{bmatrix} M_1 + h_{\mathrm{tot},1} - h_{11} & \cdots & -h_{1m} \\ \vdots & \ddots & \vdots \\ -h_{m1} & \cdots & M_m + h_{\mathrm{tot},m} - h_{mm} \end{bmatrix} \tag{11}$$

where M_j is the modal overlap factor for the reverberant field of the jth statistical subsystem and is given as (Shorter and Langley 2005b)

$$M_j = \omega n_j \eta_j \tag{12}$$

where η_j is the damping loss factor for the jth statistical subsystem. $h_{\mathrm{tot},j}$ represents the total energy leaving the reverberant field of the jth statistical subsystem per unit modal energy density in the reverberant field of the jth statistical subsystem, and can be expressed as (Shorter and Langley 2005b)

$$h_{\mathrm{tot},j} = \frac{2}{\pi}\sum_{r,s} \mathrm{Im}\{\mathbf{D}_{\mathrm{tot},rs}\}\boldsymbol{\Upsilon}^{(j)}_{\mathrm{dir},rs} \tag{13}$$

h_{jk} represents the ensemble average input power to the direct field of the reverberant field of the kth statistical subsystem per unit modal energy density in the reverberant field of the jth statistical subsystem, and can be expressed as (Shorter and Langley 2005b)

$$h_{jk} = \frac{2}{\pi}\sum_{r,s} \mathrm{Im}\left\{\mathbf{D}^{(k)}_{\mathrm{dir},rs}\right\}\boldsymbol{\Upsilon}^{(j)}_{\mathrm{dir},rs} \tag{14}$$

The time and ensemble average input power to the jth statistical subsystem is given as (Shorter and Langley 2005b)

$$P^{\mathrm{ext}}_{\mathrm{in},j} = \frac{\omega}{2}\sum_{r,s} \mathrm{Im}\left\{\mathbf{D}^{(j)}_{\mathrm{dir},rs}\right\}\mathbf{S}^{\mathrm{ext}}_{qq,rs} \tag{15}$$

Ref. (Shorter and Langley 2005b) details the derivation of Equations (10)-(15).

The power balance equations of the statistical subsystems in Equation (10) are solved to obtain the energy of the each statistical subsystem. The energy is inserted into Equation (7) to obtain the cross-spectral response of the deterministic subsystem. The

total energy of the system can be expressed as

$$E_{\mathrm{t}} = E_{\mathrm{d}} + E_{\mathrm{s}} \tag{16}$$

where E_{d} and E_{s} are the energy of the deterministic and statistical subsystems respectively, and can be written as (Muthalif and Langley 2012)

$$E_{\mathrm{d}} = \frac{\omega^2}{2} \sum_{r,s} \mathbf{M}_{rs} \mathbf{S}_{qq,rs} \tag{17}$$

$$E_{\mathrm{s}} = \sum_{p} E_p \tag{18}$$

3 Optimization problem formulation under a specific frequency

3.1 Optimization model

We consider the optimum size parameters of the complex built-up system at a high frequency. The aim of the optimum design is to minimize the vibration level of the system. The total energy of the system under a specific frequency is taken as the objective function, and the design variables are the size parameters of the system which can be divided into two types according to the types of the subsystems. They are

1) the size parameters of the deterministic subsystems, **x**,

2) the size parameters of the statistical subsystems, **y**.

Hence, the optimization problem can be stated as

$$\left.\begin{array}{ll} \text{find} & \mathbf{x},\mathbf{y} \\ \min & E_{\mathrm{t}} = E_{\mathrm{d}} + E_{\mathrm{s}} \\ \text{s.t.} & \mathbf{x}^{\mathrm{l}} \le \mathbf{x} \le \mathbf{x}^{\mathrm{u}} \\ & \mathbf{y}^{\mathrm{l}} \le \mathbf{y} \le \mathbf{y}^{\mathrm{u}} \\ & m^{\mathrm{l}} \le m \le m^{\mathrm{u}} \end{array}\right\} \tag{19}$$

where $\mathbf{x}^{\mathrm{u}}$ and $\mathbf{x}^{\mathrm{l}}$ are vectors of the upper and lower bounds of the size parameters of the deterministic subsystems, respectively. $\mathbf{y}^{\mathrm{u}}$ and $\mathbf{y}^{\mathrm{l}}$ are vectors of the upper and lower bounds of the size parameters of the statistical subsystems, respectively. m represents the total mass of the whole system, and m^{u} and m^{l} respectively represent its upper and lower bounds.

3.2 Sensitivity analysis

The optimization model of Equation (19) is solved by a gradient-based mathematical programming algorithm, which requires sensitivity analysis of the objective function and the constraint functions with respect to the design variables. This paper derives the sensitivity equations for the response of the total energy of the system by direct differentiation. The sensitivity of the objective function with respect to the design variables depends on the sensitivities of the energy of the deterministic and statistical systems, as follows.

3.2.1 Sensitivity of the objective function with respect to the size parameters of the deterministic subsystem

According to Equation (16), the sensitivity analysis of the objective function with

respect to the size parameters $\mathbf{x}$ of the deterministic subsystem can be determined by differentiating the energy of the deterministic and statistical subsystems with respect to $\mathbf{x}$. Differentiating Equation (16) with respect to the jth size parameter of the deterministic subsystem x_j gives

$$\frac{\partial E_{\mathrm{t}}}{\partial x_j} = \frac{\partial E_{\mathrm{s}}}{\partial x_j} + \frac{\partial E_{\mathrm{d}}}{\partial x_j} \tag{20}$$

Consider the derivative of the energy of the statistical subsystem with respect to x_j. Differentiating Equation (18) with respect to x_j, and using Equation (10), $\frac{\partial E_{\mathrm{s}}}{\partial x_j}$ can be expressed as

$$\frac{\partial E_{\mathrm{s}}}{\partial x_j} = \sum_k \left(\frac{\partial \mathbf{E}}{\partial x_j} \right)_k \tag{21}$$

with

$$\frac{\partial \mathbf{E}}{\partial x_j} = \mathbf{N}\mathbf{L}^{-1} \left(\frac{\partial \mathbf{P}_{\mathrm{in}}^{\mathrm{ext}}}{\partial x_j} + \frac{\partial \mathbf{P}_{\mathrm{in}}^{\mathrm{dir}}}{\partial x_j} - \frac{\partial \mathbf{L}}{\partial x_j} \mathbf{N}^{-1} \mathbf{E} \right) \tag{22}$$

Differentiating Equation (15) with respect to x_j, the derivative of the input power to the kth statistical subsystem with respect to x_j can be written as

$$\frac{\partial P_{\mathrm{in},k}^{\mathrm{ext}}}{\partial x_j} = \frac{\omega}{2} \sum_{r,s} \left[\mathrm{Im}\left\{ \mathbf{D}_{\mathrm{dir}}^{(k)} \right\}_{rs} \left\{ \boldsymbol{\chi}_{\mathrm{d}}^{(j)} \mathbf{S}_{qq}^{\mathrm{ext}} + \left(\boldsymbol{\chi}_{\mathrm{d}}^{(j)} \mathbf{S}_{qq}^{\mathrm{ext}} \right)^{\mathrm{H}} \right\}_{rs} \right] \tag{23}$$

with

$$\boldsymbol{\chi}_{\mathrm{d}}^{(j)} = -\mathbf{D}_{\mathrm{tot}}^{-1}\frac{\partial \mathbf{D}_{\mathrm{d}}}{\partial x_j} \tag{24}$$

Differentiating Equation (11) with respect to x_j, the derivative of the influence coefficient matrix of the modal energy with respect to x_j can be written as

$$\frac{\partial \mathbf{L}}{\partial x_j} = \begin{bmatrix} \frac{\partial h_{\mathrm{tot},1}}{\partial x_j} - \frac{\partial h_{11}}{\partial x_j} & \cdots & -\frac{\partial h_{1m}}{\partial x_j} \\ \vdots & \ddots & \vdots \\ -\frac{\partial h_{m1}}{\partial x_j} & \cdots & \frac{\partial h_{\mathrm{tot},m}}{\partial x_j} - \frac{\partial h_{mm}}{\partial x_j} \end{bmatrix} \tag{25}$$

By using Equations (13) and (14), the elements of Equation (25) can be written as

$$\begin{aligned} \frac{\partial h_{\mathrm{tot},k}}{\partial x_j} = \frac{2}{\pi}\sum_{r,s}\Bigg[& \mathrm{Im}\{\mathbf{D}_{\mathrm{tot}}\}_{rs}\left\{\boldsymbol{\chi}_{\mathrm{d}}^{(j)}\boldsymbol{\Upsilon}_{\mathrm{dir}}^{(k)} + \left(\boldsymbol{\chi}_{\mathrm{d}}^{(j)}\boldsymbol{\Upsilon}_{\mathrm{dir}}^{(k)}\right)^{\mathrm{H}}\right\}_{rs} \\ & + \mathrm{Im}\left\{\frac{\partial \mathbf{D}_{\mathrm{d}}}{\partial x_j}\right\}_{rs}\left(\boldsymbol{\Upsilon}_{\mathrm{dir}}^{(k)}\right)_{rs}\Bigg] \end{aligned} \tag{26}$$

$$\frac{\partial h_{kp}}{\partial x_j} = \frac{2}{\pi}\sum_{r,s}\left[\left(\mathrm{Im}\left\{\mathbf{D}_{\mathrm{dir}}^{(p)}\right\}\right)_{rs}\left\{\boldsymbol{\chi}_{\mathrm{d}}^{(j)}\boldsymbol{\Upsilon}_{\mathrm{dir}}^{(k)} + \left(\boldsymbol{\chi}_{\mathrm{d}}^{(j)}\boldsymbol{\Upsilon}_{\mathrm{dir}}^{(k)}\right)^{\mathrm{H}}\right\}_{rs}\right] \tag{27}$$

Inserting Equations (22)-(27) into Equation (21), the derivative of the energy of the statistical subsystem with respect to x_j can be obtained.

Consider now the derivative of the energy of the deterministic subsystem with respect to x_j. Differentiating Equation (17) with respect to x_j, $\frac{\partial E_{\mathrm{d}}}{\partial x_j}$ can be expressed as

$$\frac{\partial E_{\mathrm{d}}}{\partial x_j} = \frac{\omega^2}{2}\sum_{r,s}\left(\frac{\partial \mathbf{M}}{\partial x_j}\right)_{rs}\left(\frac{\partial \mathbf{S}_{qq}}{\partial x_j}\right)_{rs} \tag{28}$$

Differentiating Equation (7) with respect to x_j, and using Equations (8) and (9) gives

$$\frac{\partial \mathbf{S}_{qq}}{\partial x_j} = \boldsymbol{\chi}_{\mathrm{d}}^{(j)} \mathbf{S}_{qq} + \left(\boldsymbol{\chi}_{\mathrm{d}}^{(j)} \mathbf{S}_{qq}\right)^{\mathrm{H}} + \mathbf{D}_{\mathrm{tot}}^{-1} \left(\sum_k \frac{\partial \alpha_k}{\partial x_j} \mathrm{Im}\left\{ \mathbf{D}_{\mathrm{dir}}^{(k)} \right\} \right) \mathbf{D}_{\mathrm{tot}}^{-\mathrm{H}} \tag{29}$$

with

$$\frac{\partial \alpha_k}{\partial x_j} = \frac{4}{\pi \omega n_k} \frac{\partial E_k}{\partial x_j} \tag{30}$$

Inserting Equations (29) and (30) into Equation (28), the derivative of the energy of the deterministic subsystem with respect to x_j can be calculated. Now using Equation (20), the sensitivity of the objective function with respect to x_j can be obtained.

3.2.2 Sensitivity of the objective function with respect to the size parameters of the statistical subsystem

According to Equation (16), the sensitivity analysis of the objective function with respect to the size parameters $\mathbf{y}$ of the statistical subsystem can be determined by differentiating the energy of the deterministic and statistical subsystems with respect to $\mathbf{y}$. Differentiating Equation (16) with respect to the jth size parameter of the kth statistical subsystem $y_j^{(k)}$ gives

$$\frac{\partial E_{\mathrm{t}}}{\partial y_j^{(k)}} = \frac{\partial E_{\mathrm{s}}}{\partial y_j^{(k)}} + \frac{\partial E_{\mathrm{d}}}{\partial y_j^{(k)}} \tag{31}$$

Consider the derivative of the energy of the statistical subsystem with respect to

$y_j^{(k)}$. Differentiating Equation (18) with respect to $y_j^{(k)}$, $\frac{\partial E_\mathrm{s}}{\partial y_j^{(k)}}$ can be written as

$$\frac{\partial E_\mathrm{s}}{\partial y_j^{(k)}} = \sum_p \left(\frac{\partial \mathbf{E}}{\partial y_j^{(k)}} \right)_p \tag{32}$$

with

$$\frac{\partial \mathbf{E}}{\partial y_j^{(k)}} = \mathbf{N}\mathbf{L}^{-1} \left(\frac{\partial \mathbf{P}_\mathrm{in}^\mathrm{ext}}{\partial y_j^{(k)}} + \frac{\partial \mathbf{P}_\mathrm{in}^\mathrm{dir}}{\partial y_j^{(k)}} - \frac{\partial \mathbf{L}}{\partial y_j^{(k)}} \mathbf{N}^{-1}\mathbf{E} \right) + \frac{\partial \mathbf{N}}{\partial y_j^{(k)}} \mathbf{N}^{-1}\mathbf{E} \tag{33}$$

Differentiating Equation (15) with respect to $y_j^{(k)}$, the derivative of the input power to the pth statistical subsystem with respect to $y_j^{(k)}$ can be written as

$$\begin{aligned} \frac{\partial P_{\mathrm{in},p}^\mathrm{ext}}{\partial y_j^{(k)}} = \frac{\omega}{2} \sum_{r,s} \Bigg[& \mathrm{Im}\left\{ \frac{\partial \mathbf{D}_\mathrm{dir}^{(p)}}{\partial y_j^{(k)}} \right\}_{rs} \left(\mathbf{S}_{qq}^\mathrm{ext} \right)_{rs} \\ & + \mathrm{Im}\left\{ \mathbf{D}_\mathrm{dir}^{(p)} \right\}_{rs} \left\{ \boldsymbol{\chi}_\mathrm{dir}^{(k,j)} \mathbf{S}_{qq}^\mathrm{ext} + \left(\boldsymbol{\chi}_\mathrm{dir}^{(k,j)} \mathbf{S}_{qq}^\mathrm{ext} \right)^\mathrm{H} \right\}_{rs} \Bigg] \end{aligned} \tag{34}$$

with

$$\boldsymbol{\chi}_\mathrm{dir}^{(k,j)} = -\mathbf{D}_\mathrm{tot}^{-1} \frac{\partial \mathbf{D}_\mathrm{dir}^{(k)}}{\partial y_j^{(k)}} \tag{35}$$

For the case of $k \neq p$, Equation (34) can be simplified as

$$\frac{\partial P_{\mathrm{in},p}^\mathrm{ext}}{\partial y_j^{(k)}} = \frac{\omega}{2} \sum_{r,s} \left[\mathrm{Im}\left\{ \mathbf{D}_\mathrm{dir}^{(p)} \right\}_{rs} \left\{ \boldsymbol{\chi}_\mathrm{dir}^{(k,j)} \mathbf{S}_{qq}^\mathrm{ext} + \left(\boldsymbol{\chi}_\mathrm{dir}^{(k,j)} \mathbf{S}_{qq}^\mathrm{ext} \right)^\mathrm{H} \right\}_{rs} \right] \tag{36}$$

Differentiating Equation (11) with respect to $y_j^{(k)}$, the derivative of the influence coefficient matrix of the modal energy with respect to $y_j^{(k)}$ can be written as

$$\frac{\partial \mathbf{L}}{\partial y_j^{(k)}} = \begin{bmatrix} \frac{\partial M_1}{\partial y_j^{(k)}} + \frac{\partial h_{\mathrm{tot},1}}{\partial y_j^{(k)}} - \frac{\partial h_{11}}{\partial y_j^{(k)}} & \cdots & -\frac{\partial h_{1m}}{\partial y_j^{(k)}} \\ \vdots & \ddots & \vdots \\ -\frac{\partial h_{m1}}{\partial y_j^{(k)}} & \cdots & \frac{\partial M_m}{\partial y_j^{(k)}} + \frac{\partial h_{\mathrm{tot},m}}{\partial y_j^{(k)}} - \frac{\partial h_{mm}}{\partial y_j^{(k)}} \end{bmatrix} \tag{37}$$

By using Equations (12)-(14), the elements of Equation (37) can be written as

$$\frac{\partial M_p}{\partial y_j^{(k)}} = \omega \frac{\partial n_p}{\partial y_j^{(k)}} \eta_p \tag{38}$$

$$\frac{\partial h_{\mathrm{tot},p}}{\partial y_j^{(k)}} = \frac{2}{\pi} \sum_{r,s} \left[\mathrm{Im}\{\mathbf{D}_{\mathrm{tot}}\}_{rs} \left\{ \boldsymbol{\chi}_{\mathrm{dir}}^{(k,j)} \boldsymbol{\Upsilon}_{\mathrm{dir}}^{(p)} + \left(\boldsymbol{\chi}_{\mathrm{dir}}^{(k,j)} \boldsymbol{\Upsilon}_{\mathrm{dir}}^{(p)} \right)^{\mathrm{H}} \right. \right. \\ \left. \left. + \mathbf{D}_{\mathrm{tot}}^{-1} \mathrm{Im} \left\{ \frac{\partial \mathbf{D}_{\mathrm{dir}}^{(p)}}{\partial y_j^{(k)}} \right\} \mathbf{D}_{\mathrm{tot}}^{-\mathrm{H}} \right\}_{rs} + \mathrm{Im} \left\{ \frac{\partial \mathbf{D}_{\mathrm{dir}}^{(k)}}{\partial y_j^{(k)}} \right\}_{rs} \left(\boldsymbol{\Upsilon}_{\mathrm{dir}}^{(p)} \right)_{rs} \right] \tag{39}$$

$$\frac{\partial h_{pn}}{\partial y_j^{(k)}} = \frac{2}{\pi} \sum_{r,s} \left[\mathrm{Im}\left\{ \mathbf{D}_{\mathrm{dir}}^{(n)} \right\}_{rs} \left\{ \boldsymbol{\chi}_{\mathrm{dir}}^{(k,j)} \boldsymbol{\Upsilon}_{\mathrm{dir}}^{(p)} + \left(\boldsymbol{\chi}_{\mathrm{dir}}^{(k,j)} \boldsymbol{\Upsilon}_{\mathrm{dir}}^{(p)} \right)^{\mathrm{H}} \right. \right. \\ \left. \left. + \mathbf{D}_{\mathrm{tot}}^{-1} \mathrm{Im} \left\{ \frac{\partial \mathbf{D}_{\mathrm{dir}}^{(p)}}{\partial y_j^{(k)}} \right\} \mathbf{D}_{\mathrm{tot}}^{-\mathrm{H}} \right\}_{rs} + \mathrm{Im} \left\{ \frac{\partial \mathbf{D}_{\mathrm{dir}}^{(n)}}{\partial y_j^{(k)}} \right\}_{rs} \left(\boldsymbol{\Upsilon}_{\mathrm{dir}}^{(p)} \right)_{rs} \right] \tag{40}$$

For case of $k \neq p$, Equations (39) and (40) can be, respectively, simplified as

$$\frac{\partial h_{\mathrm{tot},p}}{\partial y_j^{(k)}} = \frac{2}{\pi}\sum_{r,s}\left[\mathrm{Im}\{\mathbf{D}_{\mathrm{tot}}\}_{rs}\left\{\boldsymbol{\chi}_{\mathrm{dir}}^{(k,j)}\boldsymbol{\Upsilon}_{\mathrm{dir}}^{(p)} + \left(\boldsymbol{\chi}_{\mathrm{dir}}^{(k,j)}\boldsymbol{\Upsilon}_{\mathrm{dir}}^{(p)}\right)^{\mathrm{H}}\right\}_{rs} + \mathrm{Im}\left\{\frac{\partial \mathbf{D}_{\mathrm{dir}}^{(k)}}{\partial y_j^{(k)}}\right\}_{rs}\left(\boldsymbol{\Upsilon}_{\mathrm{dir}}^{(p)}\right)_{rs}\right] \tag{41}$$

$$\frac{\partial h_{pn}}{\partial y_j^{(k)}} = \frac{2}{\pi}\sum_{r,s}\left[\mathrm{Im}\left\{\mathbf{D}_{\mathrm{dir}}^{(n)}\right\}_{rs}\left\{\boldsymbol{\chi}_{\mathrm{dir}}^{(k,j)}\boldsymbol{\Upsilon}_{\mathrm{dir}}^{(p)} + \left(\boldsymbol{\chi}_{\mathrm{dir}}^{(k,j)}\boldsymbol{\Upsilon}_{\mathrm{dir}}^{(p)}\right)^{\mathrm{H}}\right\}_{rs} + \mathrm{Im}\left\{\frac{\partial \mathbf{D}_{\mathrm{dir}}^{(n)}}{\partial y_j^{(k)}}\right\}_{rs}\left(\boldsymbol{\Upsilon}_{\mathrm{dir}}^{(p)}\right)_{rs}\right] \tag{42}$$

Equation (42) can be further simplified as Equation (43) if $k \neq n$.

$$\frac{\partial h_{pn}}{\partial y_j^{(k)}} = \frac{2}{\pi}\sum_{r,s}\left[\mathrm{Im}\left\{\mathbf{D}_{\mathrm{dir}}^{(n)}\right\}_{rs}\left\{\boldsymbol{\chi}_{\mathrm{dir}}^{(k,j)}\boldsymbol{\Upsilon}_{\mathrm{dir}}^{(p)} + \left(\boldsymbol{\chi}_{\mathrm{dir}}^{(k,j)}\boldsymbol{\Upsilon}_{\mathrm{dir}}^{(p)}\right)^{\mathrm{H}}\right\}_{rs}\right] \tag{43}$$

Inserting Equations (33)-(43) into Equation (32), the derivative of the energy of the statistical subsystem with respect to $y_j^{(k)}$ can be obtained.

Consider now the derivative of the energy of the deterministic subsystem with respect to $y_j^{(k)}$. Differentiating Equation (17) with respect to $y_j^{(k)}$, $\frac{\partial E_{\mathrm{d}}}{\partial y_j^{(k)}}$ can be written as

$$\frac{\partial E_{\mathrm{d}}}{\partial y_j^{(k)}} = \frac{\omega^2}{2}\sum_{r,s} M_{rs}\left(\frac{\partial \mathbf{S}_{qq}}{\partial y_j^{(k)}}\right)_{rs} \tag{44}$$

Differentiating Equation (7) with respect to $y_j^{(k)}$, and using Equations (8) and (9) gives

$$\frac{\partial \mathbf{S}_{qq}}{\partial y_j^{(k)}} = \boldsymbol{\chi}_{\mathrm{dir}}^{(k,j)} \mathbf{S}_{qq} + \left(\boldsymbol{\chi}_{\mathrm{dir}}^{(k,j)} \mathbf{S}_{qq}\right)^{\mathrm{H}} + \boldsymbol{\Xi}^{(k,j)} \tag{45}$$

where

$$\boldsymbol{\Xi}^{(k,j)} = \mathbf{D}_{\mathrm{tot}}^{-1} \left[\sum_p \left(\frac{\partial \alpha_p}{\partial y_j^{(k)}} \mathrm{Im}\left\{ \mathbf{D}_{\mathrm{dir}}^{(p)} \right\} \right) + \alpha_k \mathrm{Im}\left\{ \frac{\partial \mathbf{D}_{\mathrm{dir}}^{(k)}}{\partial y_j^{(k)}} \right\} \right] \mathbf{D}_{\mathrm{tot}}^{-\mathrm{H}} \tag{46}$$

with

$$\frac{\partial \alpha_p}{\partial y_j^{(k)}} = \frac{4}{\pi \omega n_p^2} \left(n_p \frac{\partial E_p}{\partial y_j^{(k)}} - E_p \frac{\partial n_p}{\partial y_j^{(k)}} \right) \tag{47}$$

Inserting Equations (45)-(47) into Equation (44), the derivative of the energy of the deterministic subsystem with respect to $y_j^{(k)}$ can be calculated. Now using Equation (31), the sensitivity of the objective function with respect to $y_j^{(k)}$ can be obtained.

The sensitivities of the constraint functions with respect to design variables are also passed to the optimizer. As can be seen in Equation (19), the constraint functions have simple expressions which results in simple formulas of their sensitivities.

4 Optimization problem formulation in a given frequency band

In practical applications, the excitation frequency is often distributed over a given frequency band. A small change in the excitation frequency may lead to a significant difference of the response of the system. Hence, in general, the optimum design of the

system under a specific frequency falling in the given frequency band may not be optimal over the whole frequency band. It is necessary to consider the optimization over the whole frequency band. In this study, in order to achieve a strict control on the most critical response of the system in a given frequency band, a frequency-aggregated energy function of the system is taken as the objective function to be minimized.

4.1 Optimization model

Considering n selected sampling points $\omega_k\ (k = 1,2,\dots,n)$ in the given frequency band, the maximum system energy can be expressed as $\tilde{E}_{\mathrm{t}} = \max\left(E_{\mathrm{t}}^{(1)}, E_{\mathrm{t}}^{(2)}, \cdots, E_{\mathrm{t}}^{(n)}\right)$. Hence, the optimization problem of Equation (19) can be stated as

$$\left.\begin{array}{ll} \text{find} & \mathbf{x}, \mathbf{y} \\ \min & \tilde{E}_{\mathrm{t}} = \max\left(E_{\mathrm{t}}^{(1)}, E_{\mathrm{t}}^{(2)}, \cdots, E_{\mathrm{t}}^{(n)}\right) \\ \text{s.t.} & \mathbf{x}^{\mathrm{l}} \le \mathbf{x} \le \mathbf{x}^{\mathrm{u}} \\ & \mathbf{y}^{\mathrm{l}} \le \mathbf{y} \le \mathbf{y}^{\mathrm{u}} \\ & m^{\mathrm{l}} \le m \le m^{\mathrm{u}} \end{array}\right\} \tag{48}$$

The objective function in Equation (48) is a non-smooth one, and so difficulties of convergence may occur when a gradient-based optimization algorithm is used to solve such a problem. In this paper, an approximate envelope of the objective function of the optimization model of Equation (48) is proposed as a new objective function by using the K-S function (Kreisselmeier and Steinhauser 1979). The new objective function is smooth, continuous and differentiable and can be written as

$$\tilde{E}_{\mathrm{t}} = \mathrm{KS}\left[E_{\mathrm{t}}^{(1)}, E_{\mathrm{t}}^{(2)}, \ldots, E_{\mathrm{t}}^{(n)}\right] = \frac{1}{\eta}\ln\left[\sum_{j=1}^{n} \mathrm{e}^{\eta E_{\mathrm{t}}^{(j)}}\right] \tag{49}$$

where η is the aggregation parameter. The new objective function will approach $\tilde{E}_{\mathrm{t}}$ when η takes a reasonably large value (Wrenn 1989). Therefore, the optimization model can be rewritten as

$$\left.\begin{array}{ll} \text{find} & \mathbf{x}, \mathbf{y} \\ \min & \tilde{E}_{\mathrm{t}} = \dfrac{1}{\eta}\ln\left[\displaystyle\sum_{j=1}^{n} \mathrm{e}^{\eta E_{\mathrm{t}}^{(j)}}\right] \\ \text{s.t.} & \mathbf{x}^{\mathrm{l}} \le \mathbf{x} \le \mathbf{x}^{\mathrm{u}} \\ & \mathbf{y}^{\mathrm{l}} \le \mathbf{y} \le \mathbf{y}^{\mathrm{u}} \\ & m^{\mathrm{l}} \le m \le m^{\mathrm{u}} \end{array}\right\} \tag{50}$$

4.2 Sensitivity analysis

The sensitivity analysis of the objective function of the optimization model of Equation (50) with respect to the design variables can be obtained by using the direct differentiation method. Differentiating Equation (49) with respect to the kth size parameter of the deterministic subsystem x_k gives

$$\frac{\partial \tilde{E}_{\mathrm{t}}}{\partial x_k} = \frac{\sum_{j=1}^{n}\left(\dfrac{\partial E_{\mathrm{t}}^{(j)}}{\partial x_k}\mathrm{e}^{\eta E_{\mathrm{t}}^{(j)}}\right)}{\sum_{j=1}^{n}\mathrm{e}^{\eta E_{\mathrm{t}}^{(j)}}} \tag{51}$$

As can be seen in Equation (51), the sensitivity of the objective function $\tilde{E}_{\mathrm{t}}$ in Equation (50) with respect to the kth size parameter of the deterministic subsystem can be easily obtained by using the formulations derived in section 3.2.1.

Similarly, the sensitivity of $\tilde{E}_{\mathrm{t}}$ with respect to the kth size parameter of the statistical subsystem can also be easily obtained by using the formulations derived in section 3.2.2. As mentioned in section 3.2, the sensitivities of the constraint functions with respect to the design variables can be easily obtained.

5 Numerical examples

5.1 Optimization under a specific frequency

In this section, the proposed optimization model is illustrated on a hybrid model consisting of two thin plates, one of which is taken as deterministic and the other as statistical, as shown in Figure 1. The deterministic and statistical plates are coupled via a spring whose stiffness is 10^6N/m. Properties of the plates employed in this hybrid model are given in Table 1. The edges of the deterministic plate are all simply supported. A unit excitation force is applied on the deterministic plate, with the frequency $f_{\mathrm{p}} = 200$Hz.

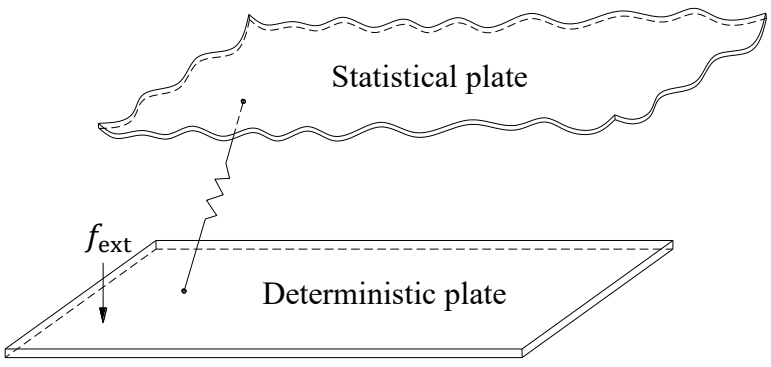

Figure 1. A hybrid model consisting of two plates coupled via a spring.

Table 1. Properties of the plates used in the hybrid model

Properties	Deterministic plate	Statistical plate
Length (m)	0.5	1.0
Width (m)	0.2	0.6
Thickness (m)	0.001	0.0015 (Initial value)
Density (kg/m^3)	7800.0	2700.0
Young's modulus (Pa)	2.0×10^{11}	7.1×10^{10}
Loss factor	0.05	0.03
Poisson's ratio	0.3	0.3

The thickness of the statistical plate b is taken as the design variable, and its upper and lower bounds are set to b^{u} =2mm and b^{l} =0.4mm, respectively. The partition of the system can be performed based on the mode numbers of the statistical and deterministic plates in the frequency range. The statistical and deterministic plates respectively have 33 and 11 non-rigid-body modes in the frequency range of 0-200Hz. Since the modal densities of the statistical and deterministic plates are significantly different, this system exhibits mid-frequency vibration behavior, and the statistical plate can remain statistical while the deterministic plate can remain deterministic over the whole optimization process.

The energy of the statistical plate is taken as the objective function. The optimization

problem is formulated as

$$\left.\begin{array}{ll} \text{find} & b \\ \min & E_{\mathrm{s}} \\ \text{s.t.} & b^{\mathrm{l}} \le b \le b^{\mathrm{u}} \end{array}\right\} \tag{52}$$

The optimization model of Equation (52) can be viewed as a special case of Equation (50). Therefore, the sensitivity analysis can be performed by using the formulations derived in section 3.

In order to verify the efficiency and effectiveness of the present sensitivity analysis method, the derivatives of the statistical plate energy with respect to its thickness obtained by using the proposed sensitivity analysis scheme and the Finite Difference Method (FDM) with 10^{-4}mm perturbation are shown in Figure 2. As can be seen, the results from two methods have good agreement. Moreover, the computational time taken for the proposed method (97s) is about half that for the FDM (195s).

The design variable is initially set to be $b_{\mathrm{Init}}=1.5$mm. A Sequential Quadratic Programming (SQP) optimizer is employed here for solving the optimization problem, and the iterative process is terminated when the relative difference between the adjacent energies of the statistical plate is less than 10^{-6}. The optimization process converged after 2 iterations as shown in Figure 3. As can be seen, the energy of the statistical plate has decreased by about 6dB (ref. 10^{-12}J).

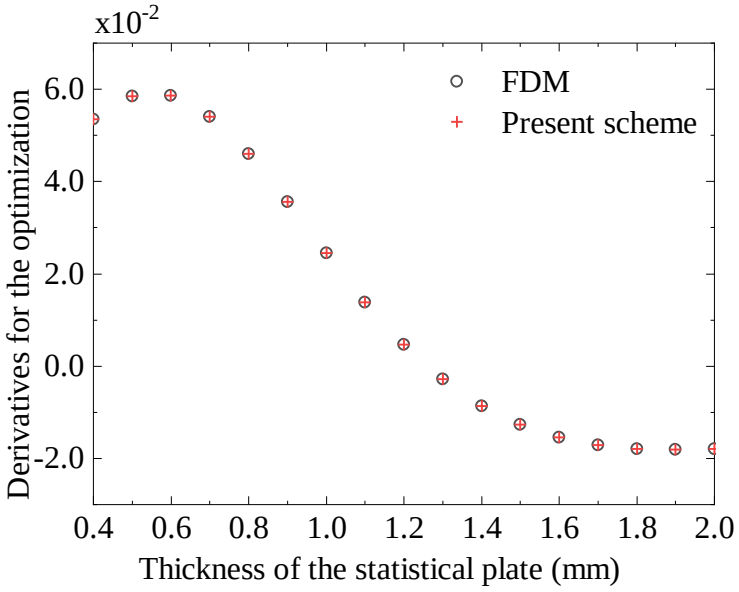

Figure 2. Derivatives of the statistical plate energy with respect to its thickness obtained using the present sensitivity analysis scheme and FDM.

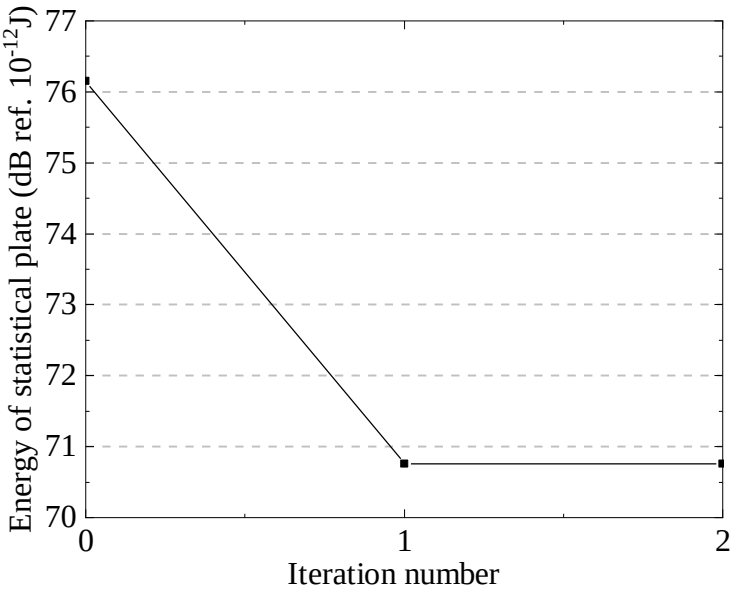

Figure 3. Iteration history of the objective function.

As a very simple optimization model, Equation (52) has only one design variable.

Hence, the energy of the statistical plate can easily be plotted against thickness, as shown in Figure 4. As can be seen, the optimum design was quickly obtained through the optimization. However, it is necessary to note that the dynamic optimization problem for a complex built-up system is highly nonconvex. In general, the optimum design obtained with a gradient-based mathematical programming algorithm is a local optimum (Sigmund and Petersson 1998). However, such solutions may provide useful guidance at the conceptual design stage, and thus be widely used in structural design.

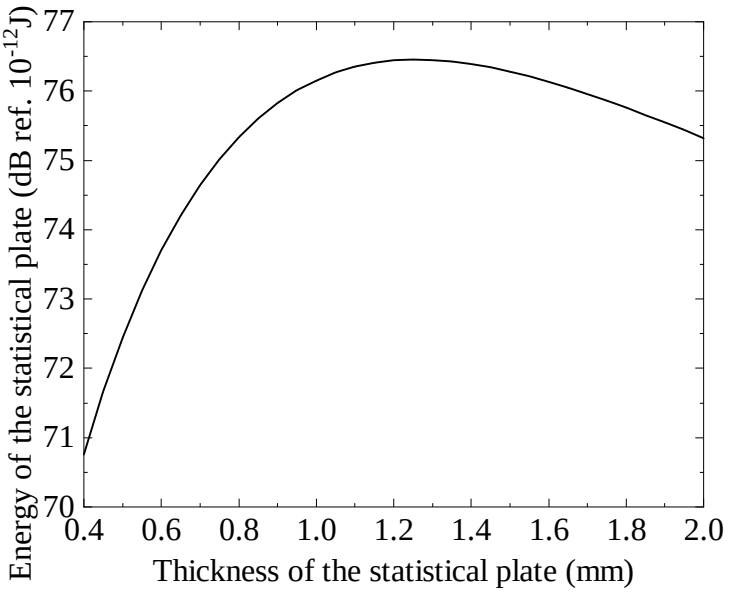

Figure 4. Energy of the statistical plate under its different thickness.

5.2 Optimization in a given frequency band

In order to verify the effectiveness of the optimization model proposed in section 4, we now consider a beam-plate system consisting of a framework combined by 10 beams

with different cross sections and a thin plate as shown in Figure 5. The framework and plate are welded together at 24 intersections of beams, and the radii of all connection points are assumed to be 1mm. The material of all beams is steel, with mass density ρ_{b} =7800.0 kg/m^3, Young's modulus E_{b} =200.0 GPa and Poisson's ratio ν_{b} =0.33. The beams numbered 1-4 in Figure 5 have length 1.0m, while those numbered 5-10 have length 0.6m. The cross sections of all beams are rectangular and have the same width (0.01m), but different heights. The material of the plate is aluminum, with mass density ρ_{p} =2700.0 kg/m^3, Young's modulus E_{p} =71.0 GPa and Poisson's ratio ν_{p} =0.33. The plate has length 1.0m and width 0.6m, and the in-plane deformation of the plate is ignored. The loss factor of all beams and the plate are all 0.5%. A unit excitation force is applied at a point on the framework as shown in Figure 5, and the frequency range considered is from 200Hz to 400Hz.

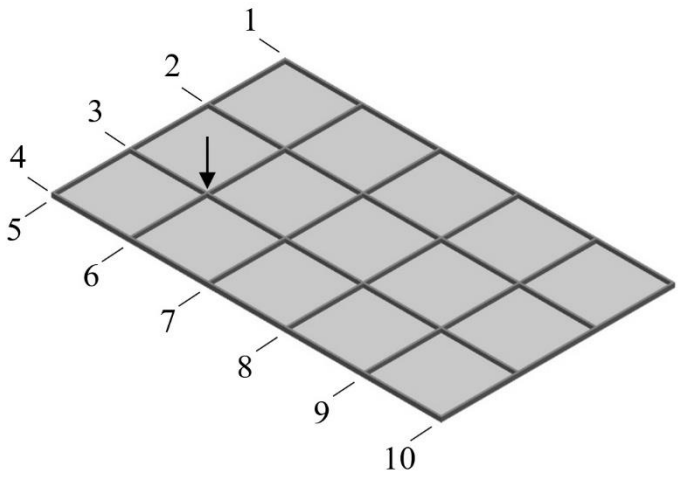

Figure 5. A beam-plate system consisting of a framework and a thin plate.

The frequency-aggregated energy of the system in a given frequency band is taken as the objective function to be minimized, and the heights of the cross sections of all beams and the thickness of the plate are taken as the design variables. The lower and upper bounds of the beam cross section heights are respectively 10mm and 50mm, while those of the plate thickness are respectively 0.5mm and 1.0mm. The upper limit of the system mass is set as 60% of the system mass when all design variables are at their upper bounds, i.e. specifying a mass constraint factor $\beta = 0.6$.

The partition of the system can be performed based on the mode numbers of the framework and the thin plate in the frequency range of interest. The thin plate and the framework respectively have 46 and 8 modes in the frequency range of 200-400Hz. Since the modal densities of the thin plate and the framework are significantly different, this system exhibits mid-frequency vibration behavior. The framework consisting of beams should be defined as the deterministic subsystem and modeled using the FE method, while the plate should be defined as the statistical subsystem and modeled using SEA. Here, the framework is discretized by Timoshenko beam elements with an element size of 25mm.

In this optimization problem, there are 11 design variables consisting of 10 and 1 plate thickness. Selecting 21 equidistant sampling frequencies in the frequency band of interest, the objective function is constructed by using Equation (49) with the aggregation parameter $\eta = 10000$. Therefore, the optimization problem can be stated as

$$\left.\begin{array}{ll} \text{find} & \mathbf{h}, b \\ \min & \tilde{E}_{\mathrm{t}} = \dfrac{1}{\eta}\ln\left[\displaystyle\sum_{j=1}^{n} \mathrm{e}^{\eta E_{\mathrm{t}}^{(j)}}\right] \\ \text{s.t.} & \mathbf{h}^{\mathrm{l}} \le \mathbf{h} \le \mathbf{h}^{\mathrm{u}} \\ & b^{\mathrm{l}} \le b \le b^{\mathrm{u}} \\ & m^{\mathrm{l}} \le m \le m^{\mathrm{u}} \end{array}\right\} \tag{52}$$

where $\mathbf{h}$ is the vector of the beam cross section heights and b is the plate thickness. The iterative process will be terminated when the relative difference between the adjacent energies of the statistical plate is less than 10^{-6}.

Consider now the sensitivity analysis of the present optimization model. For verification purposes, setting all the beam cross section heights to 20mm, and the plate thickness to 0.6mm, the derivatives of the objective function with respect to the design variables, obtained by using the present sensitivity analysis scheme and the FDM with 10^{-4}mm perturbation, are given in Figure 6 and show good agreement. The computational time for the present method (320s) is less than 10% of that for the FDM (3573s).

The initial values of the beam cross section heights are now set to 30mm, and the plate thickness is set to 0.8mm. This optimization problem is solved by using the SQP optimizer. The optimization process converged after 29 iterations as shown in Figure 7. As can be seen, the objective function first shows an upward trend, then decreases steadily, and eventually stops at a level less than its initial value, while the mass of the system is always decreasing. The initial mass of the system equals 61% of that with all design variables set to their upper bounds, and therefore does not satisfy the mass constraint

β =0.6. The first iteration pulls the system mass back to the feasible region but with a sacrifice of the objective function. However, in the following iterations the objective function decreases steadily.

Table 2. The optimized design variables.

Design variables	h_1	h_2	h_3	h_4	h_5	h_6	h_7	h_8	h_9	h_{10}	b
Values (mm)	39.2	47.5	50.0	38.0	10.0	10.0	10.0	13.1	10.0	10.0	0.5

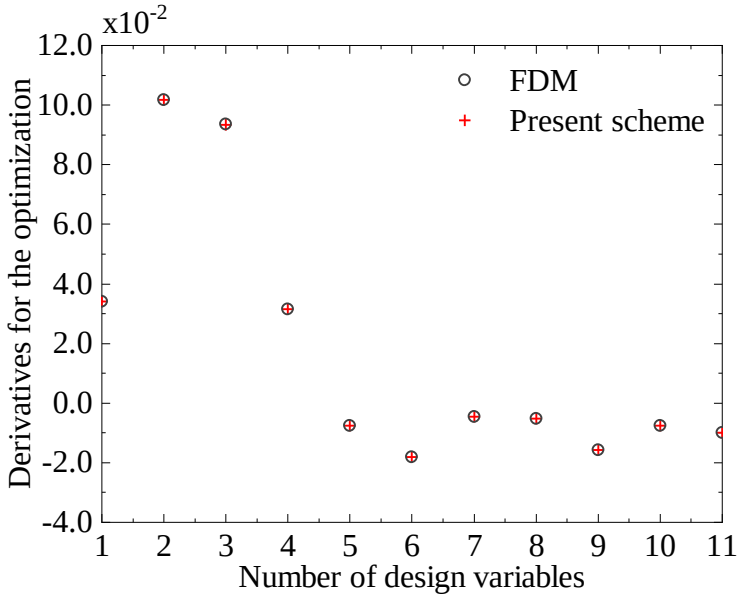

Figure 6. Derivatives of the objective function with respect to the design variables obtained using the present sensitivity analysis scheme and FDM.

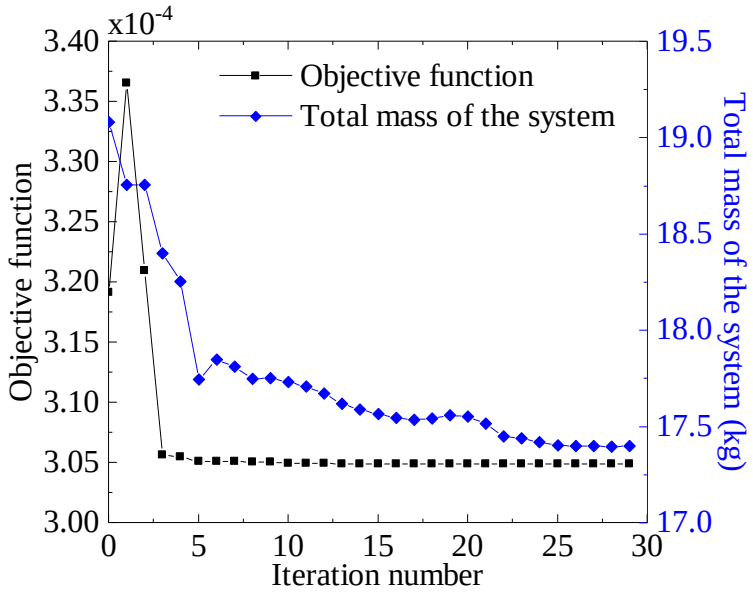

Figure 7. Iteration histories of the objective function and the mass of the system.

The final optimum design variables are given in Table 2. It can be seen that the cross section heights of the beams numbered 1-4 increase by different amounts, while those of the beams numbered 5-10 decrease significantly, mainly to their lower bounds. The thickness of the plate is also decreased to its lower bound. Figure 8 compares the total energies of the system under the different frequencies in the given frequency band for the initial and the optimum designs. As can be seen, the energy level of the system has been improved at most of the frequencies in the given frequency band except in the vicinity of 305Hz, which proves the validity of the present optimization method. It also can be seen in Figure 8 that optimization of the size parameters leads to a change in the natural frequencies of the system.

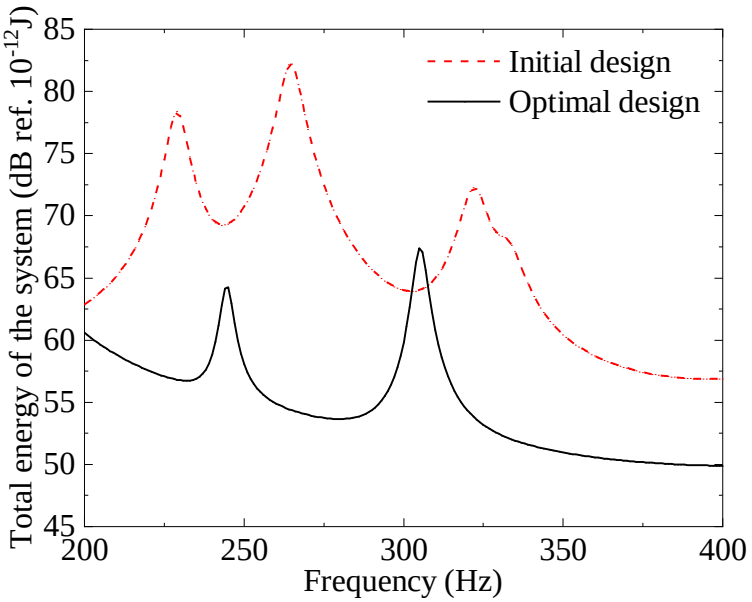

Figure 8. Energies of the system under different frequencies in the given frequency band for the initial and the optimum designs.

Figure 9 shows the energies of the framework and the plate under different frequencies in the given frequency band for the initial and optimum designs. As can be seen, the energies of both the framework and the plate are significantly decreased after optimization. The increase of the total system energy near 305Hz is mainly caused by an increase of the plate energy. The energy of the framework and the plate are very close at the peak for both the initial and optimum designs. Moreover, the energy level of the plate is higher than that of the framework over the whole frequency band both for the initial and the optimum designs, which illustrates that although the framework is the main load-bearing member, the influence of the plate should not be ignored when the beam-plate system exhibits mixed mid-frequency behavior.

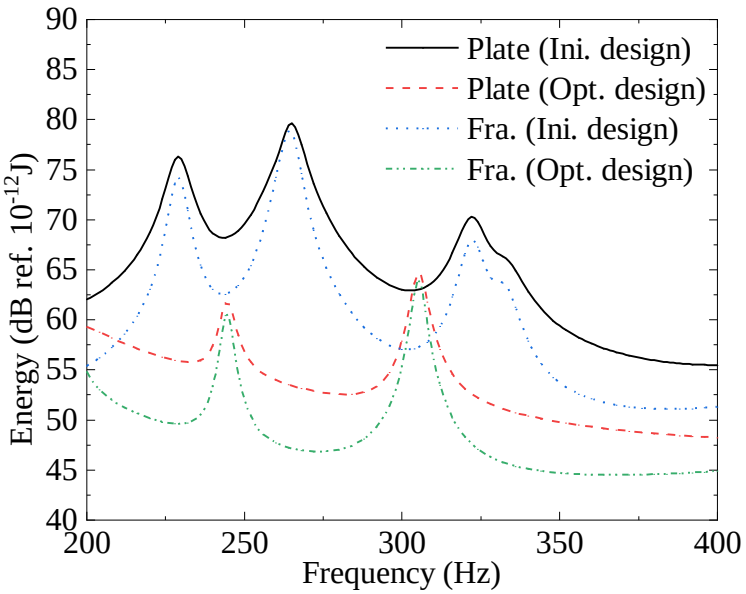

Figure 9. Energies of the framework and the plate under different frequencies in the given frequency band for the initial and the optimum designs.

Next, consider the influence of the mass constraint factor on the optimum solutions. The optimization process is performed with five different mass constraint factors (β =0.4, 0.5, 0.6, 0.7 and 0.8). The energies of the system at different frequencies in the given frequency band for the five different optimum designs are shown in Figure 10. It is found that the energy levels of the system for the five optimum designs are all lower than that for the initial design at most of the frequencies in the given frequency band. The optimum design corresponding to β =0.6 is the best of all the optimum designs. The same optimum design is obtained with the mass constraint factor set to β =0.7 and β =0.8. Therefore, when the mass constraint coefficient is greater than 0.6, the energy level of the

system cannot be improved even if structural material is added. To study the intermediate behavior of the optimal solution between β =0.6 and β =0.7, the optimization program is executed with the mass constraint factor β =0.65. The energies of the system at different frequencies in the given frequency band for the obtained optimum designs are shown in Figure 11. As can be seen, the energy curve for the optimum designs under mass constraint factor β =0.65 has the same trend as that under mass constraint factor β =0.7. However, the former has fewer peaks than the latter, especially after 300Hz.

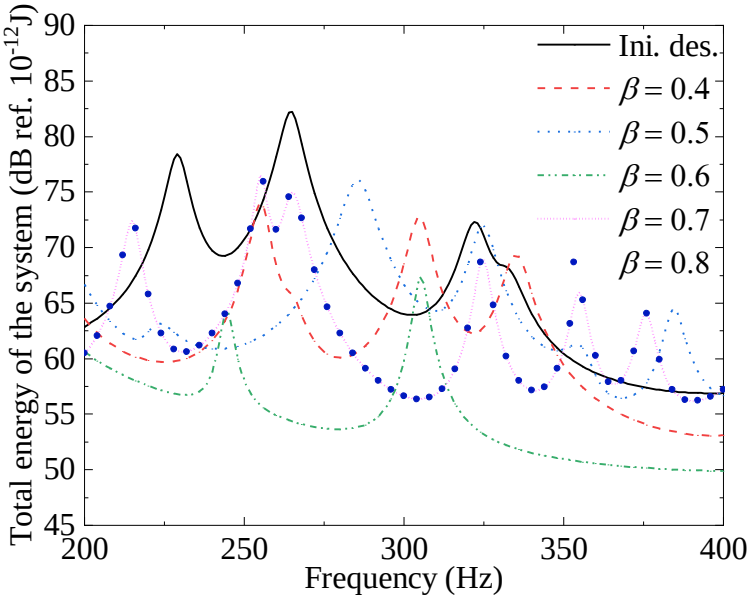

Figure 10. Energies of the system under different frequencies in the given frequency band for the initial and the optimum designs with different mass constraint factors.

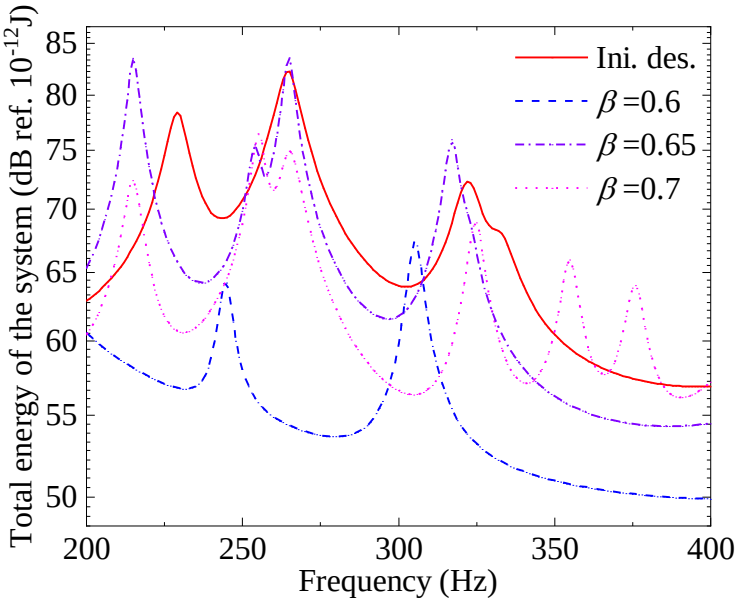

Figure 11. Energies of the system under different frequencies in the given frequency band for the initial and the optimum designs with different mass constraint factors between 0.6 and 0.7.

6 Conclusions

The sensitivity analysis of dynamic response and optimal size design of complex built-up systems in mid-frequency range are studied in this paper. By using the hybrid FE-SEA method, which combines FE and SEA as an effective method for the mid-frequency vibration of a complex built-up system, the optimization model of the system at a specific frequency or in a given frequency band is established. An efficient direct differentiation method for sensitivity analysis is derived. The optimization problem is solved by using a gradient-based mathematical programming algorithm. The efficiency and effectiveness of the proposed method are verified by two numerical examples. The

energy level of a complex built-up system, whether at a single frequency or in a given frequency band, can be significantly improved through optimization. The influence of the mass constraint factor on the optimum design is also discussed, and the results show that when the mass reaches a certain level, an increase of material is not beneficial to improving the energy level of the system.

Disclosure statement

No potential conflict of interest was reported by the authors.

Funding

The authors are grateful for support under grants from the National Natural Science Foundation of China (11672060), and the Cardiff University Advanced Chinese Engineering Centre.

References

Afimiwala, K. A., and R. W. Mayne. 1974. “Evaluation of Optimization Techniques for Applications in Engineering Design.” *Journal of Spacecraft and Rockets* 11 (10): 673-674.

Bathe, K. J. 1996. *Finite Element Procedures*. Upper Saddle River: Prentice Hall.

Bendsøe, M. P., and O. Sigmund. 2003. *Topology Optimization, Theory, Methods and*

Applications. Berlin: Springer.

Cicirello, A., and R. S. Langley. 2013. “The Vibro-Acoustic Analysis of Built-up Systems Using a Hybrid Method with Parametric and Non-Parametric Uncertainties.” *Journal of Sound and Vibration* 332 (9): 2165-2178.

Cicirello, A., and R. S. Langley. 2014. “Efficient Parametric Uncertainty Analysis within the Hybrid Finite Element/Statistical Energy Analysis Method.” *Journal of Sound and Vibration* 333 (6): 1698-1717.

Cotoni, V., P. Shorter, and R. Langley. 2007. “Numerical and Experimental Validation of a Finite Element - Statistical Energy Analysis Method.” *Journal of the Acoustical Society of America* 122 (1): 259-270.

Desmet, W. 2002. “Mid-Frequency Vibro-Acoustic Modelling: Challenges and Potential Solutions.” *Proceedings of 2002 International Conference on Noise and Vibration Engineering, ISMA*, 835-862.

Du, J., and N. Olhoff. 2007. “Minimization of Sound Radiation from Vibrating Bi-Material Structures Using Topology Optimization.” *Structural and Multidisciplinary Optimization* 33 (4-5): 305-321.

Duhamel, D., B. R. Mace, and M. J. Brennan. 2006. “Finite Element Analysis of the Vibrations of Waveguides and Periodic Structures.” *Journal of Sound and Vibration* 294: 205-220.

Dühring, M. B., J. S. Jensen, and O. Sigmund. 2008. “Acoustic Design by Topology

Optimization." *Journal of Sound and Vibration* 317 (3-5): 557-575.

Harari, I., and D. Avraham. 1997. "High-Order Finite Element Methods for Acoustic Problems." *Journal of Computational Acoustics* 5 (1): 33-51.

Hinke, L., F. Dohnal, B. R. Mace, T. P. Waters, and N. S. Ferguson. 2009. "Component Mode Synthesis as a Framework for Uncertainty Analysis." *Journal of Sound and Vibration* 324 (1-2): 161-178.

Hsieh, C. C., and J. S. Arora. 1984. "Design Sensitivity Analysis and Optimization of Dynamic Response." *Computer Methods in Applied Mechanics and Engineering* 43 (2): 195-219.

Ji, L., B. R. Mace, and R. J. Pinnington. 2006. "A Mode-Based Approach for the Mid-Frequency Vibration Analysis of Coupled Long- and Short-Wavelength Structures." *Journal of Sound and Vibration* 289 (1-2): 148-170.

Kang, B. S., G. J. Park, and J. S. Arora. 2006. "A Review of Optimization of Structures Subjected to Transient Loads." *Structural and Multidisciplinary Optimization* 31 (2): 81-95.

Karnopp, D. C., and A. K. Trikha. 1969. "Comparative Study of Optimization Techniques for Shock and Vibration Isolation." *ASME Journal of Engineering for Industry* 91 (4): 1128-1132.

Kassem, M., C. Soize, and L. Gagliardini. 2011. "Structural Partitioning of Complex Structures in the Medium-Frequency Range. An Application to an Automotive Vehicle."

Journal of Sound and Vibration 330 (5): 937-946.

Keane, A. J., and W. G. Price. 1987. “Statistical Energy Analysis of Strongly Coupled Systems.” *Journal of Sound and Vibration* 117 (2): 363-386.

Kreisselmeier, G., and R. Steinhauser. 1979. “Systematic Control Design by Optimizing a Vector Performance Index.” *Proceedings of the International Federation of Active Control Symposium on Computer Aided Design of Control Systems*, 113-117.

Ladevèze, P., and L. Arnaud. 2000. “New Computational Method for Structural Vibrations in the Medium-Frequency Range.” *Computer Assisted Mechanics and Engineering Sciences* 7 (2): 219-226.

Langley, R. S. 1989. “A General Derivation of the Statistical Energy Analysis Equations for Coupled Dynamic Systems.” *Journal of Sound and Vibration* 135 (3): 499-508.

Langley, R. S. 1989. “Application of the Dynamic Stiffness Method to the Free and Forced Vibrations of Aircraft Panels.” *Journal of Sound and Vibration* 135 (2): 319-331.

Langley, R. S. 1992. “A Wave Intensity Technique for the Analysis of High Frequency Vibrations.” *Journal of Sound and Vibration* 159 (3): 483-502.

Langley, R. S., and V. Cotoni. 2007. “Response Variance Prediction for Uncertain Vibro-Acoustic Systems Using a Hybrid Deterministic-Statistical Method.” *Journal of the Acoustical Society of America* 122 (6): 3445-3463.

Le Bot, A. 1998. “A vibroacoustic model for high frequency analysis.” *Journal of Sound and Vibration* 211 (4): 537-554.

Lyon, R. H., and R.G. DeJong. 1995. *Theory and Application of Statistical Energy Analysis.* 2nd ed. Boston: Butterworth-Heinemann.

Ma, Y., Y. Zhang, and D. Kennedy. 2015. "A Hybrid Wave Propagation and Statistical Energy Analysis on the Mid-Frequency Vibration of Built-up Plate Systems." *Journal of Sound and Vibration* 352: 63-79.

Ma, Y., Y. Zhang, and D. Kennedy. 2015. "A Symplectic Analytical Wave Based Method for the Wave Propagation and Steady State Forced Vibration of Rectangular Thin Plates." *Journal of Sound and Vibration* 339: 196-214.

Mace, B. R. 1994. "On the Statistical Energy Analysis Hypothesis of Coupling Power Proportionality and Some Implications of Its Failure." *Journal of Sound and Vibration* 178 (1): 95-112.

Mace, B. R. 2005. "Statistical Energy Analysis: Coupling Loss Factors, Indirect Coupling and System Modes." *Journal of Sound and Vibration* 279 (1-2): 141-170.

Mace, B. R., and P. J. Shorter. 2000. "Energy Flow Models from Finite Element Analysis." *Journal of Sound and Vibration* 233 (3): 369-389.

Maxit, L., and J. L. Guyader. 2003. "Extension of SEA Model to Subsystems with Non-Uniform Modal Energy Distribution." *Journal of Sound and Vibration* 265 (2): 337-358.

Muthalif, A. G. A., and R. S. Langley. 2012. "Active Control of High-Frequency Vibration: Optimisation Using the Hybrid Modelling Method." *Journal of Sound and*

Vibration 331 (13): 2969-2983.

Pluymers, B., B. Van Hal, D. Vandepitte, and W. Desmet. 2007. "Trefftz-Based Methods for Time-Harmonic Acoustics." *Archives of Computational Methods in Engineering* 14 (4): 343-381.

Sevin, E., and W. D. Pilkey. 1971. *Optimal Shock and Vibration Isolation*. United States Department of Defence: The Shock and Vibration Information Centre.

Shorter, P. J., and R. S. Langley. 2005a. "On the Reciprocity Relationship between Direct Field Radiation and Diffuse Reverberant Loading." *Journal of the Acoustical Society of America* 117 (1): 85-95.

Shorter, P. J., and R.S. Langley. 2005b. "Vibro-Acoustic Analysis of Complex Systems." *Journal of Sound and Vibration* 288 (3): 669-699.

Sigmund, O., and J. Petersson. 1998. "Numerical Instabilities in Topology Optimization: A Survey on Procedures Dealing with Checkerboards, Mesh-Dependencies and Local Minima." *Structural Optimization* 16 (1): 68-75.

Soize, C. 1998. "Reduced Models in the Medium-Frequency Range for General External Structural-Acoustic Systems." *Journal of the Acoustical Society of America* 103 (6): 3393-3406.

Tanner, G. 2009. "Dynamical energy analysis - determining wave energy distribution in vibro-acoustical structures in the high-frequency regime." *Journal of Sound and Vibration* 320 (4-5): 1023-1038.

Taylor, J. E. 1968. “Optimum Design of a Vibrating Bar with Specified Minimum Cross Section.” *AIAA Journal* 6 (7): 1379-1381.

Van Vinckenroy, G., and W. P. De Wilde. 1995. “The Use of Monte Carlo Techniques in Statistical Finite Element Methods for the Determination of the Structural Behavior of Composite Materials Structural Components.” *Composite Structures* 32 (1-4): 247-253.

Vanmarcke, E., and M. Grigoriu. 1983. “Stochastic Finite Element Analysis of Simple Beams.” *ASCE Journal of Engineering Mechanics* 109 (5): 1203-1214.

Vergote, K., B. Van Genechten, D. Vandepitte, and W. Desmet. 2011. “On the Analysis of Vibro-Acoustic Systems in the Mid-Frequency Range Using a Hybrid Deterministic-Statistical Approach.” *Computers and Structures* 89 (11-12): 868-877.

Wilcox, L. C., G. Stadler, C. Burstedde, and O. Ghattas. 2010. “A High-Order Discontinuous Galerkin Method for Wave Propagation through Coupled Elastic-Acoustic Media.” *Journal of Computational Physics* 229 (24): 9373-9396.

Wrenn, G. A. 1989. “An Indirect Method for Numerical Optimization Using the Kreisselmeier-Steinhauser Function.” *NASA Technical Report CR-4220, NASA.*

Yamazaki, F., M. Shinozuka, and G. Dasgupta. 1988. “Neumann Expansion for Stochastic Finite Element Analysis.” *ASCE Journal of Engineering Mechanics* 114 (8): 1335-1354.

Zarghamee, M. S. 1968. “Optimum Frequency of Structures.” *AIAA Journal* 6 (4): 749-

750.

Zhang, X., and Z. Kang. 2014. “Dynamic Topology Optimization of Piezoelectric Structures with Active Control for Reducing Transient Response.” *Computer Methods in Applied Mechanics and Engineering* 281 (1): 200-219.

Zhao, X., and N. Vlahopoulos. 2000. “Hybrid Finite Element Formulation for Mid-Frequency Analysis of Systems with Excitation Applied on Short Members.” *Journal of Sound and Vibration* 237 (2): 181-202.

Zhu, D., H. Chen, X. Kong, and W. Zhang. 2014. “A Hybrid Finite Element-Energy Finite Element Method for Mid-Frequency Vibrations of Built-up Structures under Multi-Distributed Loadings.” *Journal of Sound and Vibration* 333 (22): 5723-5745.

Zienkiewicz, O. C., and R. L. Taylor. 2000. *The Finite Element Method*. 5th ed. Boston: Butterworth-Heinemann.